arXiv:1408.1216v1 [cond-mat.mtrl-sci] 6 Aug 2014

Half metallic ferromagnetism in tri-layered perovskites $Sr_4T_3O_{10}$ (T=Co, Rh)

Madhav P. Ghimire[1,2], R. K. Thapa[3], D. P. Rai[3], Sandeep[3], T. P. Sinha[4] and Xiao Hu[2]

[1] Nepal Academy of Science and Technology, P. O. Box 3323, Khumaltar, Lalitpur, Nepal
[2] International Center for Materials Nanoarchitectonics (WPI-MANA), National Institute for Materials Science, Tsukuba 305-0044, Japan
[3] Department of Physics, Mizoram University, Aizawl 796-004, India
[4] Department of Physics, Bose Institute, Kolkata 796-004, India

E-mail: Hu.Xiao@nims.go.jp

Abstract. First-principles density functional theory (DFT) is used to investigate the electronic and magnetic properties of $Sr_4Rh_3O_{10}$, a member of the Ruddlesden-Popper series. Based on the DFT calculations taking into account the co-operative effect of Coulomb interaction (U) and spin-orbit couplings (SOC), $Sr_4Rh_3O_{10}$ is found to be a half metallic ferromagnet (HMF) with total angular moment $\mu_{\rm tot}$=12μ_B per unit cell. The material has almost 100% spin-polarization at the Fermi level despite of sizable SOC. Replacement of Rh atom by the isovalent Co atom is considered. Upon full-replacement of Co, a low-spin to intermediate spin transition happens resulting in a HMF state with the total angular moment three-time larger (i.e. $\mu_{\rm tot}$=36μ_B per unit cell), compared to $Sr_4Rh_3O_{10}$. We propose $Sr_4Rh_3O_{10}$ and $Sr_4Co_3O_{10}$ as candidates of half metals.

PACS numbers: 85.75.-d, 75.70.Tj, 75.50.Cc, 71.15.Mb

1. Introduction

The emerging developments of magneto-electronic devices have intensified research on novel materials that can be applied as a single-spin electron sources and high-efficiency magnetic sensors [1]. One of the key points to achieve such materials is to manipulate the spin polarization by band engineering. Half metals (HMs) are one class of promising materials which are metallic in one spin channel, while insulating in the opposite spin channel due to the asymmetric band structures. HMs can generate fully spin-polarized currents without any external operation [2, 3]. Ideally HM is specified by integer spin magnetization in units of Bohr magneton, where the total number of electrons per unit cell is an integer and all valence bands are fully filled in the insulating spin channel. HM states have been identified in several groups of materials which includes oxides (CrO_2), mixed-valent manganites ($La_{1-x}A_xMnO_3$ where A=Ca, Ba, Sr), Heusler alloys (NiMnSb), perovskites (Sr_2FeTO_6, where T=Mo, Re), etc. [4–18].

A recent study on layered-perovskites belonging to the Ruddlesden-Popper (RP) series [19] exhibits novel properties desirable in spintronics [9]. In cobaltates, the single-layered compound Sr_2CoO_4 shows ferromagnetic (FM) as well as HM behavior [20, 21]. The same material is reported to show negative magnetoresistance [22]. $La_{1+x}Sr_{2-x}Mn_2O_7$ is found to exhibit colossal magnetoresistance (CMR) [23] while its nonstoichiometric samples shows novel microstructural features [24]. In ruthenates, the change in number n of RuO_2 layers leads to a variety of collective phenomena: spin-triplet chiral superconductivity [25] ($n = 1$); heavy d-electron masses [26] ($n = 2, 3$), CMR effects [27] ($n = 2$) and itinerant ferromagnetism and metamagnetism ($n = 3$) [28, 29] as well as HM ferromagnetism ($n = \infty$) [30]. Furthermore, the delicate interplay between electron-electron correlation and spin-orbit coupling (SOC) in iridates gives rise to various unconventional phases. Insulator-metal transition was observed in $Sr_{n+1}Ir_nO_{3n+1}$ with increasing n [31]. Sr_2IrO_4 and $Sr_3Ir_2O_7$ have been realized as a $J_{\text{eff}} = 1/2$ Mott-insulator evidenced by an experiment [31–35] whereas, $SrIrO_3$ is a paramagnetic metal [35].

A newly synthesized tri-layered rhodate $Sr_4Rh_3O_{10}$ [36] belonging to Sr-Rh-O family in the RP series [19] comes into our attention with the unique properties. The crystal with general formula $Sr_{n+1}Rh_nO_{3n+1}$ (where $n = 3$) is built up by regular intergrowth of rock-salt Sr-O sheets and perovskites $(SrRhO_3)_n$. Rh atoms carry on charge state +4 with spin magnetizations, and the material exhibits strong crystal distortion due to rotation and tilting of the octahedra. With a total of 68 atoms in its unit cell, the system has four formula units. The other member in the series includes well studied compounds such as Sr_2RhO_4, $Sr_3Rh_2O_7$, and $SrRhO_3$ [37–42].

In this study, we investigate for the first-time the electronic and magnetic properties of $Sr_4Rh_3O_{10}$ by using first-principles density functional theory (DFT). The ground-state of $Sr_4Rh_3O_{10}$ is found to be a half-metallic ferromagnet (HMF). With an integer total angular moment $\mu_{\text{tot}} = 12\mu_B$ per unit cell, the HM state is robust to strong electron-correlation and SOC effects. Replacement of Rh by Co atoms is considered in $Sr_4Rh_3O_{10}$. For full replacement, the material $Sr_4Co_3O_{10}$ is a HMF with total magnetization increasing by three times of magnitude due to intermediate spin configuration. The insulating state of $Sr_4Co_3O_{10}$ flips to the opposite spin channel in contrast with $Sr_4Rh_3O_{10}$.

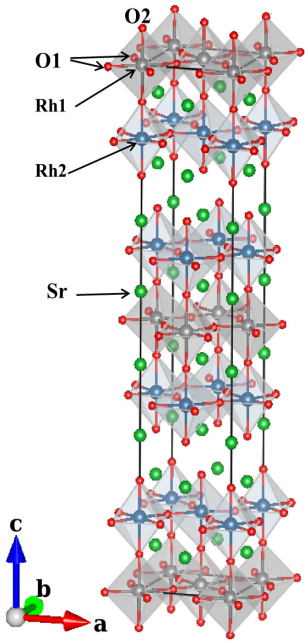

Figure 1. Crystal structure of the tri-layered perovskite $Sr_4Rh_3O_{10}$. O1 (planar) and O2 (apical) are the oxygen bonded to Rh ions forming RhO_6 octahedron.

2. Crystal structures and methods

$Sr_4Rh_3O_{10}$ crystallizes in an orthorhombic structure with space group *Pbam* as shown in figure 1. The unit cell is composed of triple layers of corner-shared RhO_6 octahedra separated by double rock-salt layers of Sr-O. Each layer is formed independently by two types of Rh atoms as shown in figure 1. In the crystal of $Sr_4Rh_3O_{10}$ two inequivalent oxygen atoms were found along the plane (O1) and along the apex (O2). The bond-lengths between Rh and planar (1.98Å) and apical (2.02Å) oxygens are different due to tilting and rotation of RhO_6 octahedron. The amplitude of rotation of RhO_6 octahedra estimated from experiments [36] is $\sim$12° which is close to that of $Sr_3Rh_2O_7$ (10.5°) [41].

The electronic structure calculations were performed by using the full-potential linearized augmented plane wave plus local orbital method implemented in the WIEN2k code [43]. The atomic sphere radii ($R_{\rm MT}$) were 2.2, 2.07, 1.97 and 1.7 Bohr for Sr, Rh, Co, and O respectively. The standard generalized gradient approximation (GGA) exchange-correlation potential within the Perdew-Burke-Ernzerhof scheme [44] were used. The results presented below are for Coulomb interaction [45] U=3 and 5eV for Rh and Co, respectively, and we have confirmed that the main conclusions do not change with $U = 1 \sim 5$eV for Rh and $U = 4.2 \sim 8$eV for Co [46]. The SOC was considered via second variational method using the scalar-relativistic orbitals as basis. Starting from the experimental results [36], we optimize the lattice parameters to determine the equilibrium positions of all the individual atoms and reach the stable structure using WIEN2k code [43] with the force convergence set at 1mRy/a.u. All the presented results are of the optimized structure tabulated in table 1, which agrees

Table 1. Optimized atomic coordinates for $Sr_4Rh_3O_{10}$ obtained by minimizing the total energy from first principles DFT calculations.

Atom	x	y	z
Sr1	0.5	0.0	0.0697
Sr2	0.5	0.0	0.2047
Sr3	0.0	0.0	0.2953
Sr4	0.0	0.0	0.4303
Rh1	0.0	0.0	0.0
Rh2	0.0	0.0	0.14
Rh3	0.5	0.0	0.354
Rh4	0.5	0.0	0.5
O1	0.3135	0.1866	0.0
O2	0.1919	0.3081	0.1391
O3	0.3080	0.3081	0.3609
O4	0.1865	0.1866	0.5
O5	0.0	0.0	0.0689
O6	0.0	0.0	0.21
O7	0.5	0.0	0.2899
O8	0.5	0.0	0.4311

with the results obtained from the experimental lattice parameters [36].

3. Parent material $Sr_4Rh_3O_{10}$

In the ionic picture, Rh with five d-electrons nominally has a charge state +4. The five $4d$ electrons occupy the t_{2g} triplet and leave the higher e_g doublet empty due to large crystal-field generated by oxygen octahedron. The low-spin alignment of Rh is then $t_{2g}^3\uparrow$, $t_{2g}^2\downarrow$ giving rise to a moment of $1\mu_B$/atom.

In order to know the ground state electronic and magnetic structures of $Sr_4Rh_3O_{10}$, we perform the DFT calculations considering the co-operative effect of U and SOC. The ground state is found to be ferromagnetic (FM) with the lowest energy among other magnetic configurations. To compare the relative effect from U and SOC, the total density of states (DOS) are plotted in figure 2 with GGA, GGA+U and GGA+U+SO functional. Within GGA functional, $Sr_4Rh_3O_{10}$ shows metallic characters for both spin-up and spin-down channels. For $U \geq$ 1eV, the topmost valence band in spin-up channel shifts deeper towards the valence region giving rise to an insulating state. In contrary, for spin-down channel the metallic state is maintained, except that the DOS peak near $E_{\rm F}$ is splitted due to strong electron-correlations. The effect of U is comparatively small as expected due to partial occupation of the orbitals in spin-down channel. With spin-up channel insulating (band-gap 0.9eV) and the spin-down channel metallic, $Sr_4Rh_3O_{10}$ is a half-metal (HM). It is generally considered that the presence of heavy element with strong SOC strength might destroy the HM state. In the present case it turns out that the HM state is fully preserved even with SOC as observed in figure 2(c). This happens due to the large-exchange splitting between the spin-up and spin-down bands at $E_{\rm F}$.

As revealed by the site-projected DOS shown in figure 3 for spin-up and spin-down channels obtained from first-principles calculations within GGA+U+SO, two

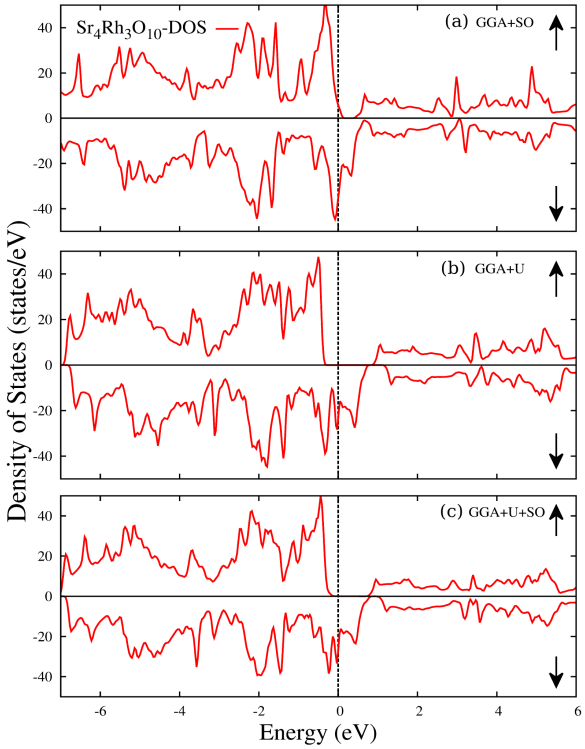

Figure 2. Total DOS for $Sr_4Rh_3O_{10}$ within (a) GGA+SO, (b) GGA+U, and (c) GGA+U+SO, respectively.

in-equivalent Rh ions play significant role in dictating the electronic properties of $Sr_4Rh_3O_{10}$. The crystal field effect is found prominent in Rh which causes the splitting between t_{2g} and e_g states. The partial DOS contribution from d states of two in-equivalent Rh atoms shows full occupation of the t_{2g} states with its sub-level d_{xy} and $d_{xz}+d_{yz}$ lying below $E_{\rm F}$, whereas the e_g states are in the conduction region for spin-up channel. For spin-down channel, the t_{2g} states are partially occupied due to deficiency of one electron in the $d_{xz}+d_{yz}$ sub-levels. As a result, these bands cross $E_{\rm F}$ and form a continuous band at $E_{\rm F}$. The order of occupation observed in figure 3 is consistent with the ionic picture. The crystal-field energy ($\sim$1.3eV) is close to the exchange energy splitting ($\sim$1.2eV) between spin-up and spin-down bands of Rh atoms. This clearly indicates the low-spin configuration consistent with the ionic picture.

As shown in figure 3, Rh1 has a dominant t_{2g} characters near $E_{\rm F}$ with an itinerant DOS due to its strong hybridization with the oxygen atoms. On the other hand Rh2 has a sharp peak near $E_{\rm F}$ contributed by d_{xy} states since the hybridization with the oxygen is relatively weak unlike the $d_{xz}+d_{yz}$ states. This occurs mainly due to crystal distortion in $Sr_4Rh_3O_{10}$. Since the hybridization of Rh with the planar oxygen (O1) is stronger than apical oxygen (O2) in both spin channels, the moment induced at O1 is larger than O2 (see table 2).

To distinguish the effect of SOC, we show the spin-resolved band structure for

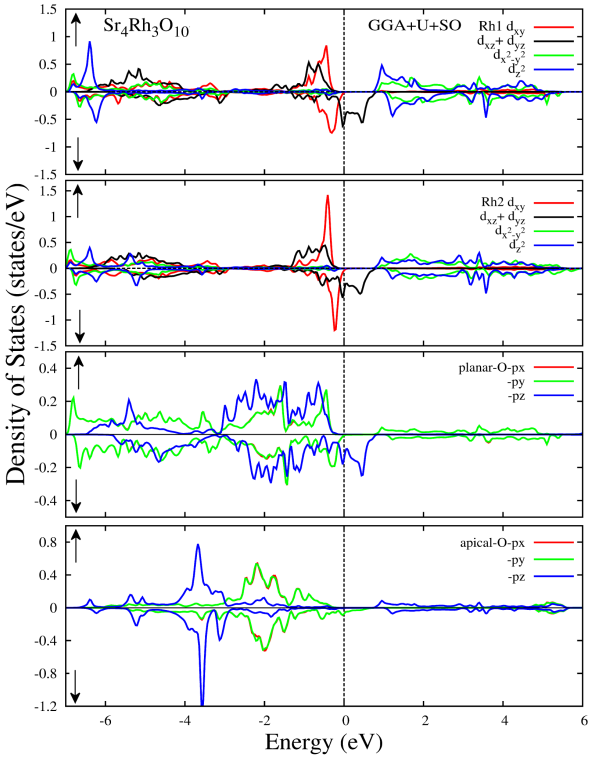

Figure 3. Partial density of states for two in-equivalent Rh-4*d* states and contributions from planar as well as apical oxygen-2*p* states in spin-up (↑) and spin-down (↓) channels for $Sr_4Rh_3O_{10}$ within GGA+*U*+SO.

$Sr_4Rh_3O_{10}$ within GGA+*U* and GGA+*U*+SO as shown in figure 4, together with a schematic diagram of the band ordering of Rh-*d* states. First we look at the gap between spin-up and spin-down channel in the conduction region for GGA+*U*. The gap is found to be ∼0.1eV at high symmetry point Γ in the Brillouin zone (BZ) (see figure 4(left)). When SOC is considered, the electronic band structure is modified. The major changes are observed in the conduction region above 0.7eV and in the valence region below -0.3eV. Due to SOC effect of Rh (ζ =191meV) [39], the spin-up bands in the conduction region at $\sim$ 0.7eV are pushed up towards higher energy by the spin-down bands. This generates a gap of $\sim$ 0.24eV at the high symmetry point Γ in the conduction region (see figure 4(right)). Similar changes are observed below E_F around -0.3eV, where the spin-up bands are pushed deeper in the valence region. Thus, the bands at E_F are purely of spin-down channel. This shows that HM state is fully preserved in $Sr_4Rh_3O_{10}$ even though sizable SOC exists.

At the ground state obtained from first-principles calculations, the total angular moment (μ_{tot}) is $12\mu_B$ per unit cell contributed by Rh atoms and oxygen atoms (see table 2). The orbital contribution in Rh ($\sim 0.1\mu_B$) is in accordance with the Hund's third rule, where Rh with more than half-filled t_{2g}-shell has its orbital moment parallel to its spin moment. The Rh moment is less than unity, with the remaining part

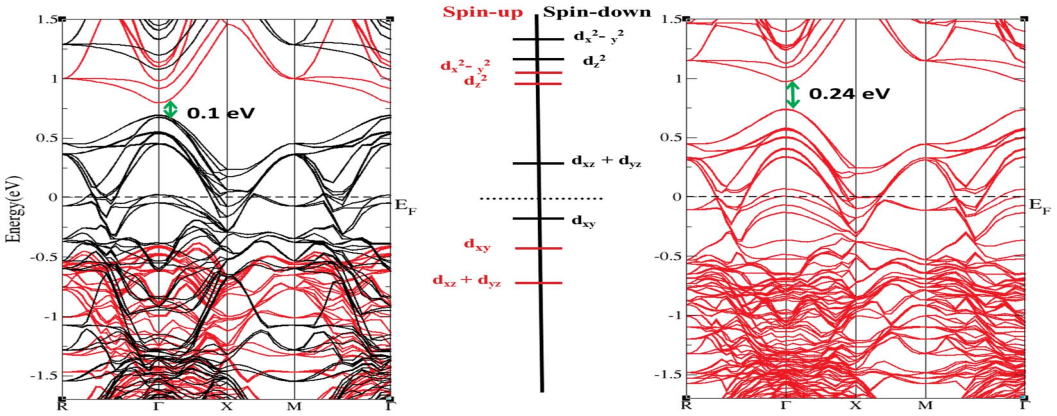

Figure 4. Band structures for $Sr_4Rh_3O_{10}$ within GGA+U (left) and GGA+U+SO (right) approach. Schematic band-diagram (middle) demonstrates the contribution from Rh-d bands in the band structure for GGA+U. Bands in red (black) within GGA+U indicates spin up (down) channel.

Table 2. Moments per atom of Rh and Co, one set of two in-equivalent oxygen atoms and unit cell ($\mu_{\rm tot}$) for $Sr_4T_3O_{10}$ (where T=Rh, Co) from first-principles calculations within GGA+U+SO. The unit of moments is the Bohr magneton $\mu_{\rm B}$. The contributions from individual atoms are within muffin-tins while the total moment includes those from the interstitial regime.

	T1	T2	O1	O2	$\mu_{\rm tot}$
$Sr_4Rh_3O_{10}$	0.63	0.54	0.11	0.05	12
$Sr_4Co_3O_{10}$	2.65	2.68	0.02	0.18	36

transferred to oxygen due to strong hybridization as seen from the partial DOS (see figure 3). Planar oxygen atoms have higher moment than the apical oxygen due to shorter bond-length with Rh-ions. In an ionic picture, each Rh ion carries moment $+1\mu_{\rm B}$ giving rise to $\mu_{\rm tot} = 12 \times (+1\mu_{\rm B}) = 12\mu_{\rm B}$ in a unit cell, consistent with the first-principles calculations.

4. Doped material $Sr_4Co_3O_{10}$

We consider the replacement of Rh by Co atoms, which corresponds to iso-valent doping into the parent material $Sr_4Rh_3O_{10}$. In the ionic picture Co retains the charge state +4. The spin state transforms from low-spin of $Sr_4Rh_3O_{10}$ to intermediate-spin $t_{2g}^3\uparrow, d_{3z^2-r^2}^1\uparrow, d_{xy}^1\downarrow$. The spin-state transition is observed frequently in cobaltates [47].

We focus on the most interesting case (i.e. full-replacement of Rh by Co atoms) where HM state is achieved.

From the total and partial DOS of $Sr_4Co_3O_{10}$ shown in figure 5, the material has full occupation of the t_{2g} states and partial occupation of the e_g states resulting to

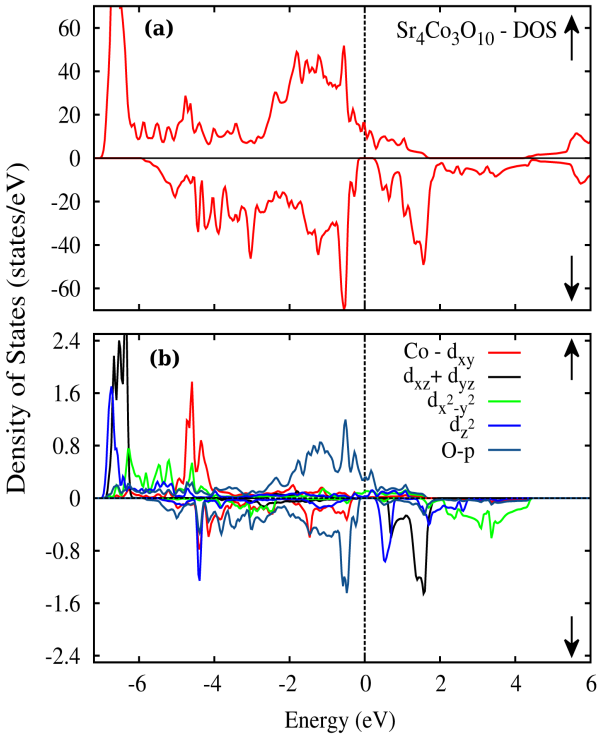

Figure 5. Density of states for $Sr_4Co_3O_{10}$ in spin-up (↑) and spin-down (↓) channels within GGA+U+SO: (a) total; (b) partial contribution from Co-d and O-$p$orbitals.

a metallic state in spin-up channel. In spin-down channel, d_{xy} state is fully occupied whereas the remaining t_{2g} and e_g states lie in the conduction region. This gives rise to band-gap of ∼0.5eV in spin-down channel. Due to crystal distortion the d states of Co hybridize strongly with the O-2p states in both spin-channels. It is interesting to note that doping of Co flips the insulating state from spin-up to spin-down channel due to intermediate-spin configuration of Co in $Sr_4Co_3O_{10}$ [46]. Thus, with metallic state in spin-up channel and the insulating state in spin-down channel, the material $Sr_4Co_3O_{10}$ is a HM.

From the first-principles calculations, the total angular moment is found to be $\mu_{\rm tot} = 36\mu_{\rm B}$ per unit cell. The moments of Co atoms and oxygen atoms are shown in table 2.

5. Discussions

First-principles calculations on magnetic anisotropy energy of $Sr_4Rh_3O_{10}$ and $Sr_4Co_3O_{10}$ indicate the c axis of the crystal as their easy axis with anisotropy energy of $\sim$ 3meV and $\sim$ 0.95meV per unit cell, respectively.

SOC mixes the spin-up and spin-down electrons together which possibly destroys the HM state. In the present materials the exchange-splitting between the spin-up and spin-down DOS at $E_{\rm F}$ is large (see figures 2 and 5), which makes the mixing

marginally small at E_F. Hence, HM state is preserved even with SOC.

From our calculations, the material $Sr_4Rh_3O_{10}$ has larger exchange splitting which reduces the mixing of spin-up and spin-down bands at E_F, and its low total moment causes a small stray field generated by local magnetic ions. Hence compared to $Sr_4Co_3O_{10}$ with a three-time larger moment, $Sr_4Rh_3O_{10}$ is more desirable as a HMF.

6. Conclusions

Based on the first-principles density functional approach, $Sr_4Rh_3O_{10}$ is found to be a half metallic ferromagnet due to the cooperative effect from Coulomb interaction, spin-orbit coupling and the crystal field. It is demonstrated that doping iso-valent atom into the system by replacing Rh with Co, a half metal with larger moment is achieved. It is emphasized that the large exchange splitting between spin-up and spin-down bands at the Fermi level retains the half metallicity even in presence of spin-orbit coupling.

Acknowledgments

MPG thanks M. Richter, IFW-Dresden for valuable discussions and suggestions and the organizers of FPLO-2013 for financial support to present this work. MPG acknowledges the partial support from NAST (Nepal) and INSA (India) under the NAST-INSA bilateral exchange program. This work was supported partially by WPI Initiative on Materials Nanoarchitectonics, MEXT, Japan.

References

[1] Wolf S A, Awschalom D D, Buhrman R A, Daughton J M, von Molnar S, Roukes M L, Chtchelkanova A Y and Treger D M 2001 Spintronics: A spin-based electronics vision for the future *Science* **294** 1488

[2] de Groot R A, Mueller F M, van Engen P G and Buschow K H J 1983 New class of materials: Half-metallic ferromagnets *Phys. Rev. Lett.* **50** 2024

[3] Pickett W E and Moodera J S 2001 Half metallic magnets *Physics Today* **54** 39

[4] Schwarz, K 1986 CrO_2 predicted as a half-metallic ferromagnet *J. Phys. F Met. Phys.* **16** L211

[5] Pickett W E 1998 Spin-density-functional-based search for half-metallic antiferromagnets *Phys. Rev. B* **57** 10613

[6] Kobayashi K -I, Kimura T, Sawada H, Terakura K and Tokura Y 1998 Room-temperature magnetoresistance in an oxide material with an ordered double-perovskite structure *Nature (London)* **395** 677

[7] Sarma D D, Mahadevan P, Saha-Dasgupta T, Ray S and Kumar A 2000 Electronic structure of Sr_2FeMoO_6 *Phys. Rev. Lett.* **85** 2549

[8] Dowben P A and Skomski R 2003 Finite-temperature spin polarization in half-metallic ferromagnets *J. Appl. Phys.* **93** 7948

[9] Felser C, Fecher G H and Balke B 2007 Spintronics: A challenge for materials science and solid-state chemistry *Angew. Chem. Int. Ed.* **46** 668

[10] Hu X 2012 Half-metallic antiferromagnet as a prospective material for spintronics *Adv. Mater.* **24** 294

[11] Wan X, Kohno M and Hu X 2005 Orbital order and ferrimagnetic properties of $Sr_8CaRe_3Cu_4O_{24}$ *Phys. Rev. Lett.* **94** 087205; Wan X, Kohno M and Hu X 2005 Robust half-metallic character and large oxygen magnetism in a perovskite cuprate *Phys. Rev. Lett.* **95** 146602

[12] Galanakis I, Mavropoulos Ph and Dederichs P H 2006 Electronic structure and SlaterPauling behaviour in half-metallic Heusler alloys calculated from first principles *J. Phys. D: Appl. Phys.* **39** 765

[13] Sargolzaei M, Richter M, Koepernik K, Opahle I, Eschrig H 2006 Spin and orbital magnetism in full Heusler alloys: A density functional theory study of Co_2YZ (Y=Mn,Fe; Z=Al,Si,Ga,Ge) *Phys. Rev. B* **74** 224410

[14] Kandpal H C, Fecher G H and Felser C. 2007 Calculated electronic and magnetic properties of the half-metallic, transition metal based Heusler compounds *J. Phys. D: Appl. Phys.* **40** 1507

[15] Katsnelson M I, Irkhin Y Yu, Chioncel L, Lichtenstein A I and de Groot R A 2008 Half-metallic ferromagnets: From band structure to many-body effects *Rev. Mod. Phys.* **80** 315

[16] Müller G M, Walowski J, Djordjevic M, Miao G -X, Gupta A, Ramos A V, Gehrke K, Moshnyaga V, Samwer K, Schmalhorst J, Thomas A, Hütten A, Reiss G, Moodera J S and Münzenberg M 2009 Spin polarization in half-metals probed by femtosecond spin excitation *Nat. Mater.* **8** 56

[17] Ghimire M P, Sandeep, Sinha T P and Thapa R K 2011 First principles study of the electronic and magnetic properties of semi-Heusler alloys NiXSb (X = Ti, V, Cr and Mn) *J. Alloys Compd.* **509** 9742

[18] Ghimire M P, Wu L -H and Hu X 2014 Possible half metallic antiferromagnetism in a double perovskite material with strong spin-orbit couplings *arXiv*:1407.3408

[19] Ruddlesden S N and Popper P 1957 New compounds of the K_2NiF_4 type *Acta Crystallogr.* **10** 538; Ruddlesden S N and Popper P 1958 The compound $Sr_3Ti_2O_7$ and its structure *Acta Crystallogr.* **11** 54 (1958).

[20] Matsuno J, Okimoto Y, Fang Z, Yu X Z, Matsui Y, Nagaosa N, Kawasaki M and Tokura Y 2004 Metallic ferromagnet with square-lattice CoO_2 sheets *Phys. Rev. Lett.* **93** 167202

[21] Pandey S K 2010 Correlation induced half-metallicity in a ferromagnetic single-layered compound: Sr_2CoO_4 *Phys. Rev. B* **81** 035114

[22] Wang X L, Sakurai H and Muromachi E T 2005 Synthesis, structures, and magnetic properties of novel RoddlesdenPopper homologous series $Sr_{n+1}Co_nO_{3n+1}$ (n=1,2,3,4, and ∞) *J. Appl. Phys.* **97** 10M519

[23] Moritomo Y, Asamitsu A, Kuwahara H and Tokura Y 1996 Giant magnetoresistance of manganese oxides with a layered perovskite structure *Nature* **380** 141

[24] Seshadri R, Maignan A, Martin C, Letouzr F and Raveau B 1997 Magnetic and transport properties of the 1201-phase $Tl_{0.94}Sr_2Cu_{0.4}Co_{0.6}O_{5-}$ *Phys. Rev. B* **56** 5504 (1997).

[25] Mackenzie A P and Maeno Y 2003 The superconductivity of Sr_2RuO_4 and the physics of spin-triplet pairing *Rev. Mod. Phys.* **75** 657

[26] Lee J, Allan M P, Wang M A, Farrel J, Grigera S A, Baumberger F, Davis J C and Mackenzie A P 2009 Heavy *d*-electron quasiparticle interference and real-space electronic structure of $Sr_3Ru_2O_7$ *Nature Phys.* **5** 800

[27] Lin X N, Zhou Z X, Durairaj V, Schlottmann P and Cao G 2005 Colossal magnetoresistance by avoiding a ferromagnetic state in the Mott system $Ca_3Ru_2O_7$ *Phys. Rev. Lett.* **95** 017203

[28] Mao Z Q, Zhou M, Hooper J, Golub V and O'Connor C J 2006 Phase separation in the itinerant metamagnetic transition of $Sr_4Ru_3O_{10}$ *Phys. Rev. Lett.* **96** 077205

[29] Cao G, Balicas L, Song W H, Sun Y P, Xin Y, Bondarenko V A, Brill J W, Parkin S and Lin X N 2003 Competing ground states in triple-layered $Sr_4Ru_3O_{10}$: Verging on itinerant ferromagnetism with critical fluctuations *Phys. Rev. B* **68** 174409

[30] Jeng H -T, Lin S -H and Hsue C -S 2006 Orbital ordering and Jahn-Teller distortion in perovskite ruthenate $SrRuO_3$ *Phys. Rev. Lett.* **97** 067002

[31] Moon S J, Jin H, Kim K W, Choi W S, Lee Y S, Yu J, Cao G, Sumi A, Funakubo H, Bernhard C and Noh T W 2008 Dimensionality-controlled insulator-metal transition and correlated metallic state in 5*d* transition metal oxides $Sr_{n+1}Ir_nO_{3n+1}$ (n= 1, 2, and ∞) *Phys. Rev. Lett.* **101** 226402

[32] Kim B J, Jin H, Moon S J, Kim J -Y, Park B -G, Leem C S, Yu J, Noh T W, Kim C, Oh S -J, Park J -H, Durairaj V, Cao G and Rotenberg E 2008 Novel $J_{\text{eff}} = 1/2$ Mott state induced by relativistic spin-orbit coupling in Sr_2IrO_4 *Phys. Rev. Lett.* **101** 076402

[33] Kim B J, Ohsumi H, Komesu T, Sakai S, Morita T, Takagi H, Arima T 2009 Phase-sensitive observation of a spin-orbital Mott state in Sr_2IrO_4 *Science* **323** 1329

[34] Okada Y, Walkup D, Lin H, Dhital C, Chang T -R, Khadka S, Zhou W, Jeng H -T, Paranjape M, Bansil A, Wang Z, Wilson S D and Madhavan V 2013 Imaging the evolution of metallic states in a correlated iridate *Nat. Mater.* **12** 707

[35] Zhang H, Haule K and Vanderbilt D 2013 Effective $J = 1/2$ insulating state in Ruddlesden-Popper iridates: An LDA+DMFT study *Phys. Rev. Lett.* **111** 246402

[36] Yamaura K, Huang Q, Young D P and Muromachi E T 2004 Crystal structure and magnetic properties of the trilayered perovskite $Sr_4Rh_3O_{10}$: A new member of the strontium rhodate family *Chem. Mater.* **16** 3424

[37] Lee Y S, Lee J S, Noh T W, Byun D Y, Yoo K S, Yamaura K and Muromachi E T 2003 Systematic trends in the electronic structure parameters of the 4*d* transition-metal oxides $SrMO_3$(M=Zr, Mo, Ru, and Rh) *Phys. Rev. B* **67** 113101

[38] Kim B J, Yu J, Koh H, Nagai I, Ikeda S I, Oh S -J and Kim C 2006 Missing xy-band Fermi surface in 4*d* transition-metal oxide Sr_2RhO_4: Effect of the octahedral rotation on the electronic structure *Phys. Rev. Lett.* **97** 106401

[39] Haverkort M W, Elfimov I S, Tjeng L H, Sawatzky G A and Damascelli A 2008 Strong spin-orbit coupling effects on the Fermi surface of Sr_2RuO_4 and Sr_2RhO_4 *Phys. Rev. Lett.* **101** 026406

[40] Itoh M, Shimura T, Inaguma Y and Morii Y 1995 Structure of two-dimensional conductor of Sr_2RhO_4 *J. Sol. Stat. Chem.* **118** 206

[41] Yamaura K, Huang Q, Young D P, Noguchi Y and Muromachi E T 2002 Crystal structure and electronic and magnetic properties of the bilayered rhodium oxide $Sr_3Rh_2O_7$ *Phys. Rev. B* **66** 134431

[42] Yamaura K and Muromachi E T 2001 Enhanced paramagnetism of the 4*d* itinerant electrons in the rhodium oxide perovskite $SrRhO_3$ *Phys. Rev. B* **64** 224424

[43] Blaha P, Schwarz K, Madsen G K H, Kvasnicka D and Luitz J 2001 WIEN2k, *An augmented plane wave+Local orbitals program for calculating crystal properties* (Technische Universität Wien, Vienna, Austria ISBN 3-9501031-1-2)

[44] Perdew J P, Burke K and Ernzerhof M 1996 Generalized gradient approximation made simple *Phys. Rev. Lett.* **77** 3865

[45] Liechtenstein A I, Anisimov V I and Zaanen J 1995 Density-functional theory and strong interactions: Orbital ordering in Mott-Hubbard insulators *Phys. Rev. B* **52** R5467; Anisimov V I, Aryasetiawan F and Lichtenstein A I 1997 First-principles calculations of the electronic structure and spectra of strongly correlated systems: the LDA+U method *J. Phys. : Condens. Matter* **9** 767

[46] It should be noted that band gap opens for $Sr_4Co_3O_{10}$ in spin-down channel for $U_{\rm eff} \geq 4.2$eV (where $U_{\rm eff} = U - J$ with J fixed to 0.8eV).

[47] Zhang W, Koepernik K, Richter M and Eschrig H 2009 Magnetic phase transition in CoO under high pressure: A challenge for LSDA+U *Phys. Rev. B* **79** 155123